

Temperature dependent resistance of magnetic tunnel junctions as a quality proof of the barrier

U. Rüdiger,^{a)} R. Calarco, U. May, K. Samm, J. Hauch, H. Kittur, M. Sperlich, and G. Güntherodt

II. Phys. Institut, RWTH Aachen, 52056 Aachen, Germany

Tunnel junctions of Co(10 nm)/AlO_x (nominally 2 nm)/Co(20 nm) have been prepared by molecular beam epitaxy applying a shadow mask technique in conjunction with an UV light-assisted oxidation process of the AlO_x barrier. The quality of the AlO_x barrier has been proven by x-ray photoelectron spectroscopy and temperature dependent tunneling magnetoresistance (TMR) measurements. Optimum-oxidized tunnel junctions show a TMR of 20% at 285 K and up to 36% at 100 K. At 285 K the TMR values as a function of oxidation time are not symmetric about the optimum time. For underoxidized junctions the TMR is reduced more strongly than for overoxidized junctions. The temperature dependence of the junction's resistance is a clear and reliable indicator whether pinholes (or imperfections) contribute to the conduction across the barrier.

Magnetic tunnel junctions (MTJs) consisting of two ferromagnetic electrodes separated by a thin insulating layer (typical AlO_x) show large tunnel magnetoresistance (TMR) at room temperature making them promising candidates for magnetic random access memory (MRAM) devices.¹⁻³ Strong efforts have been spent on reducing the resistance \times area($R\times A$) product by reducing the thickness of the typically used AlO_x insulating barrier ($<10\text{ \AA}$). But not only the thickness of the insulating barrier, but also the oxidation process itself has a significant influence on the $R\times A$ product.⁴ Different oxidation processes have been investigated and optimized in order to evaluate the efficiency and reliability for large scale oxidation of the barrier material.⁵⁻⁹ In comparison with other oxidation processes ultraviolet (UV) light-assisted oxidation^{10,11} generally leads to a factor of 10–100 lower $R\times A$ products and a significantly smaller bias dependence of the TMR for optimum oxidized samples.⁴ On the other hand, lowering the $R\times A$ product by minimizing the AlO_x barrier thickness may enhance the probability of a pinhole (or direct metal–metal contact) formation¹² in the insulating barrier. The recent observation of large MR effects in magnetic nanocontacts in the presence of trapped domain walls¹³⁻¹⁵ suggests that spin-dependent domain wall scattering¹⁶⁻¹⁸ can significantly contribute to the MR of MTJ. In order to distinguish spin-dependent tunneling conductance from conductance through pinholes the ‘‘Rowell criteria’’ can be applied.¹⁹ As recently discussed only the analysis of the temperature dependent resistance (conductance) seems to be reliable and gives an ‘‘easy-to-handle’’ control of the conduction mechanisms in MTJs.^{20,21}

In this article we discuss the optimization of the UV light-assisted oxidation process of AlO_x barriers of MBE prepared Co(10 nm)/AlO_x (2 nm)/Co(20 nm)/Si(100) junctions by controlling the oxidation process by x-ray photo-

electron spectroscopy (XPS), TMR, and the temperature dependent $R\times A$ product as a function of oxidation time.

MTJs have been fabricated by shadow mask deposition using electron beam evaporation in UHV (base pressure $p = 8\times 10^{-11}$ mbar). The area of the bottom and top Co electrodes separated by the AlO_x barrier is $(150\times 150)\text{ }\mu\text{m}^2$. The 2-nm thick Al layers have been deposited by e -beam evaporation followed by an *in situ* oxidation process in an O₂ atmosphere using a 15 W UV lamp inside the chamber. For XPS measurements the monochromatized Mg K_{α} emission line of $E = h\nu = 1253.6\text{ eV}$ has been employed. Low bias dc resistance and TMR measurements have been performed in a variable temperature high magnetic-field cryostat.

Figure 1 shows the XPS spectra of UHV prepared Al(2 nm)/Co(20 nm) double layers in the Al 2s and 2p core level region (55–135 eV). A nonoxidized Al(2 nm)/Co(20 nm) double layer acts as reference for the XPS investigation of

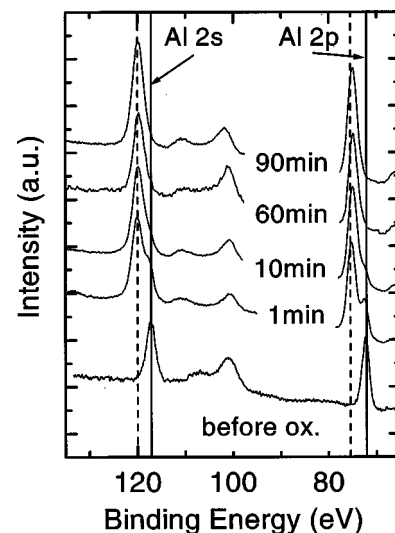


FIG. 1. XPS spectra of the Al 2s and 2p core levels of Al(2 nm)/Co(20 nm) double layers as function of oxidation time t_{ox} .

^{a)} Author to whom correspondence should be addressed; electronic mail: ruediger@physik.rwth-aachen.de

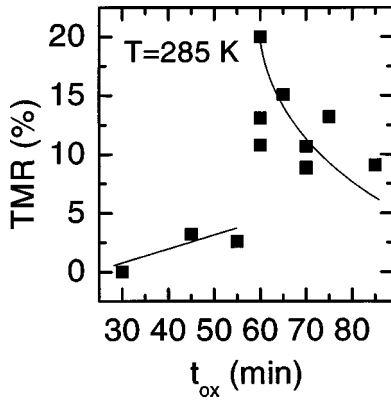


FIG. 2. Tunneling magnetoresistance of Co(10 nm)/AlO_x (2 nm)/Co(20 nm) junctions as function of oxidation time at $T=285$ K.

the oxidation process. Already after 1 min of UV light-assisted oxidation the Al $2s$ (117.2 eV) and $2p$ (72.2 eV) peaks are clearly shifted by approximately 2.1 eV. The presence of a double peak structure for both levels indicates that the Al layer is not fully oxidized. Nevertheless, most of the Al has been oxidized within the first 10 min. After 60 min of oxidation the double-peak like structure of the Al core levels disappears, indicating a fully oxidized Al layer. For oxidation times larger than 60 min the XPS spectra in the Al core level region do not change anymore. XPS Co core level ($2p_{1/2}$ and $2p_{3/2}$) spectra also support that 60 min oxidation time is the optimum oxidation time achieving a fully oxidized Al layer without oxidizing the underlying Co electrode.²²

For junctions oxidized during $t_{ox}=60$ min the TMR at $T=100$ K exhibits a sharp maximum of 36%. Slightly under- and overoxidized samples (45 and 75 min oxidation time) reveal a reduction of the TMR to approximately 20% symmetric about $t_{ox}=60$ min.

Figure 2 shows TMR values of Co(10 nm)/AlO_x (2 nm)/Co(20 nm) junctions as function of oxidation time at $T=285$ K with a maximum TMR for $t_{ox}=60$ min of approximately 20%. The $R \times A$ product for the optimum-oxidized sample is 160 ± 60 k Ω μm^2 . In contrast, the TMR values as a function of oxidation time are not symmetric about the optimum time. For underoxidized samples ($t_{ox} \leq 55$ min) the TMR is reduced more strongly than for the over-oxidized samples ($t_{ox} \geq 65$ min). For example the TMR for junctions with $t_{ox}=55$ min has been determined to be 2.5%, whereas the TMR for a sample with $t_{ox}=65$ min is still 15%. Also modestly overoxidized samples ($t_{ox}=85$ min) can show a TMR of approximately 10%.²²

The observed strong decrease of the TMR of underoxidized samples as function of temperature can have different origins. For an interpretation one has to distinguish between the temperature dependence of the spin-dependent and spin-independent contribution to the resistivity. The decrease of the spin-dependent tunneling contribution with increasing temperature is based on the reduction of the magnetization (spin polarization) of the electrodes (especially at the electrode/barrier interface) due to the excitation of magnons and due to broadening of the Fermi distribution.²³ For the

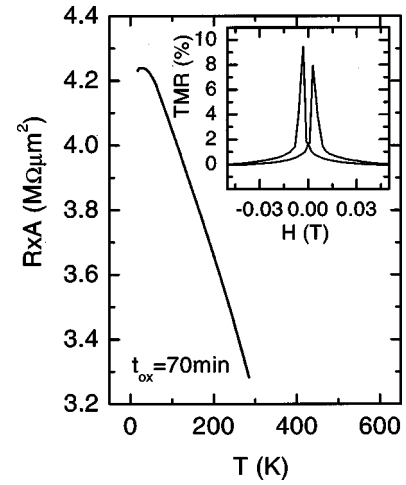


FIG. 3. The resistance \times area ($R \times A$) product of an overoxidized ($t_{ox}=70$ min) Co(10 nm)/AlO_x (2 nm)/Co(20 nm) junction exhibits an insulator-like temperature dependence. The inset shows a typical field dependent magnetoresistance curve with maxima for antiparallely magnetized electrodes (at $T=285$ K).

spin-independent contribution to the resistance a hopping process via localized states due to imperfections in the insulating barrier has been suggested.²³ Such hopping processes can give rise to a temperature dependent reduction of the TMR much faster than based on magnon excitations only.

In a simple model underoxidation leads to a very thin Al interlayer between the AlO_x and the Co bottom electrode or to Al inclusions within the already formed AlO_x barrier. In the presence of a nonuniformly oxidized barrier (Al/AlO_x double layer) or nonoxidized Al inclusions within the oxide barrier the temperature dependence of a spin-independent tunneling contribution can be larger than in the case of an overoxidized sample with an additional CoO_x layer separating the Co bottom electrode and the AlO_x barrier.²²

Additionally, a remaining Al layer on top of the Co bottom electrode can significantly reduce the surface spin polarization of the Co interface layer close to the Fermi energy E_F . Spin-polarized band structure calculations have shown that an Al termination of the Co bottom electrode strongly reduces the spin polarization of Co at the interface.^{24,25} Also randomly distributed Al inclusions can have an influence on the spin polarization of the tunneling current. With an increasing impurity concentration within the barrier the spin polarization of the tunneling current decreases, leading to a reduction of the TMR.^{26,27} Therefore, underoxidation can affect the performance of junctions more seriously than overoxidation. But it is still open why a similar asymmetric reduction of TMR at $T=100$ K for underoxidized samples has not been observed.

For interpreting the temperature dependence of the TMR data one has to keep in mind that there is no strict evidence of a full antiparallel alignment of the two Co electrodes. Different temperature dependent coercivities of the electrodes may induce different degrees of antiparallelism as a function of temperature, therefore leading to the observed asymmetric reduction of TMR at $T=285$ K.

Figure 3 shows the $R \times A$ product as a function of tem-

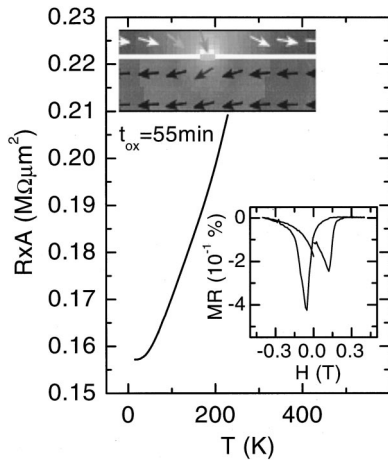


FIG. 4. The resistance \times area ($R\times A$) product of a slightly underoxidized ($t_{\text{ox}}=55$ min) Co(10 nm)/AlO_x (2 nm)/Co(20 nm) junction exhibits a metal-like temperature dependence. The bottom inset shows an unusual field dependent magnetoresistance curve, which has minima for antiparallely magnetized Co electrodes (at $T=10$ K). The top inset gives the magnetization distribution of the two Co electrodes (10 and 20 nm thick) separated by a 2-nm-thick insulator in the presence of a pinhole.

perature for an overoxidized junction ($t_{\text{ox}}=70$ min) which decreases with increasing temperature as is typical for tunnel junctions. At $T=285$ K the $R\times A$ product is approximately $3\text{ M}\Omega\ \mu\text{m}^2$. The inset of Fig. 3 shows a typical field dependent TMR curve with maxima for antiparallely magnetized electrodes.

In contrast, the $R\times A$ product of a sample showing no TMR ($t_{\text{ox}}=55$ min) increases with increasing temperature (see Fig. 4) pointing to metallic channels (pinholes) through the insulating barrier.²⁰ In contrast to the TMR curve in the inset of Fig. 3 the MR curve of this sample shows minima for antiparallely magnetized electrodes (see bottom inset of Fig. 4). Generally, all investigated MTJ with a metal-like temperature dependent resistance also exhibit comparable MR curves. These unusual TMR curves can be interpreted on the basis of anisotropic MR, which has its origin in spin-orbit coupling depending on the relative orientation of the current \mathbf{I} and the magnetization \mathbf{M} .²⁸ Generally, in ferromagnets the resistance for $\mathbf{I}\parallel\mathbf{M}$ is larger than for $\mathbf{I}\perp\mathbf{M}$ ($R_{\parallel}>R_{\perp}$).²⁸ The magnetization distribution during the magnetization reversal of the two Co electrodes (10 and 20 nm thick) separated by a 2-nm-thick insulator layer has been calculated in the presence of a 5-nm-wide pinhole and is shown in the top inset in Fig. 4 for antiparallely magnetized electrodes.²⁹ The local magnetization distribution is indicated by arrows. Due to the presence of the pinhole there is a significant perpendicular magnetization component, which probably leads to the observed reduced resistance for antiparallely magnetized electrodes.

In summary, an UV light-assisted oxidation process of Co(10 nm)/AlO_x (2 nm)/Co(20 nm) junctions has been investigated as a function of oxidation time. The TMR shows a

sharp maximum as a function of oxidation time near $t_{\text{ox}}=60$ min, but the decrease of TMR for overoxidized junctions with increasing oxidation time is less pronounced than for underoxidized junctions. For an “easy-to-control” fabrication process of tunneling junctions a slight overoxidation seems to be favorable. Temperature dependent resistance measurements are a reliable method ruling out MTJ with pinholes (direct metal-metal point contacts).

This work was supported by the German Federal Ministry for Education and Research “BMBF” under Grant No. FKZ 13N7329 and the EC TMR Program “Submicron Magnetic Structures and Magneto-Transport Devices” (SUB-MAGDEV).

- ¹ S. S. P. Parkin *et al.*, J. Appl. Phys. **85**, 5828 (1999).
- ² J. S. Moodera, L. R. Kinder, T. M. Wong, and R. Meservey, Phys. Rev. Lett. **74**, 3273 (1995).
- ³ W. J. Gallagher *et al.*, J. Appl. Phys. **81**, 3741 (1997).
- ⁴ H. Boeve, E. Girgis, J. Schelten, J. De Boeck, and G. Borghs, Appl. Phys. Lett. **76**, 1048 (2000).
- ⁵ H. Boeve, R. J. M. van de Veerdonk, B. Dutta, J. De Boeck, J. Moodera, and G. Borghs, J. Appl. Phys. **83**, 6700 (1998).
- ⁶ J. S. Moodera, L. R. Kinder, J. Nowak, P. LeClair, and R. Meservey, Appl. Phys. Lett. **69**, 708 (1996).
- ⁷ P. K. Wong, J. E. Evetts, and M. G. Blamire, J. Appl. Phys. **83**, 6697 (1998).
- ⁸ T. Miyazaki and N. Tezuka, J. Magn. Magn. Mater. **139**, 1231 (1995).
- ⁹ S. S. P. Parkin, R. E. Fontana, and A. C. Marley, J. Appl. Phys. **81**, 5521 (1997).
- ¹⁰ P. Rottländer, H. Kohlstedt, H. A. M. de Gronckel, E. Girgis, J. Schelten, and P. Grünberg, J. Magn. Magn. Mater. **210**, 251 (2000).
- ¹¹ P. Rottländer, H. Kohlstedt, P. Grünberg, and E. Girgis, J. Appl. Phys. **87**, 6067 (2000).
- ¹² R. Schad, D. Allen, G. Zangari, I. Zana, D. Yang, M. Tondra, and D. Wang, Appl. Phys. Lett. **76**, 607 (2000).
- ¹³ N. Garcia, M. Munoz, and Y. W. Zhao, Phys. Rev. Lett. **82**, 2923 (1999).
- ¹⁴ G. Tataru, Y. W. Zhao, M. Munoz, and N. Garcia, Phys. Rev. Lett. **83**, 2030 (1999).
- ¹⁵ N. Garcia, Appl. Phys. Lett. **77**, 1351 (2000).
- ¹⁶ P. M. Levy and S. Zhang, Phys. Rev. Lett. **79**, 5110 (1997).
- ¹⁷ U. Rüdiger, J. Yu, L. Thomas, S. S. P. Parkin, and A. D. Kent, Phys. Rev. B **59**, 11914 (1999).
- ¹⁸ U. Ebels, A. Radulescu, Y. Henry, L. Piraux, and K. Ounadjela, Phys. Rev. Lett. **84**, 983 (2000).
- ¹⁹ *Tunneling Phenomena in Solids*, edited by E. Burnstein and S. Lundqvist (Plenum, New York, 1969).
- ²⁰ B. J. Jönsson-Åkerman, R. Escudero, C. Leighton, S. Kim, I. K. Schuller, and D. A. Rabson, Appl. Phys. Lett. **77**, 1870 (2000).
- ²¹ D. A. Rabson, B. J. Jönsson-Åkerman, A. H. Romero, R. Escudero, C. Leighton, S. Kim, and I. K. Schuller, J. Appl. Phys. (submitted).
- ²² U. May, K. Sann, H. Kittur, J. O. Hauch, R. Calarco, U. Rüdiger, and G. Güntherodt, Appl. Phys. Lett. (submitted).
- ²³ C. H. Shang, J. Nowak, R. Jansen, and J. S. Moodera, Phys. Rev. B **58**, R2917 (1998).
- ²⁴ I. Mertig (private communication).
- ²⁵ I. I. Oleinik, E. Y. Tsymlal, and D. G. Pettifor, Phys. Rev. B **62**, 3952 (2000).
- ²⁶ E. Y. Tsymlal and D. G. Pettifor, Phys. Rev. B **58**, 432 (1998).
- ²⁷ E. Y. Tsymlal and D. G. Pettifor, J. Appl. Phys. **85**, 5801 (1999).
- ²⁸ I. Campell and A. Fert, in *Ferromagnetic Materials*, edited by E. Wohlfarth (North-Holland, Amsterdam, 1982), Vol. 3.
- ²⁹ The micromagnetic calculations have been performed using the OOMMF code from the National Institute of Standards and Technology (NIST). Details about this micromagnetic calculation will be published elsewhere.